



Published in final edited form as:

Nat Commun. 2013 ; 4: 1939. doi:10.1038/ncomms2927.

Caspase-2 is required for dendritic spine and behavioral alterations in J20 APP transgenic mice

Julio Pozueta^{1,†}, Roger Lefort^{1,†}, Elena M. Ribe², Carol M. Troy¹, Ottavio Arancio¹, and Michael Shelanski^{1,*}

¹Department of Pathology & Cell Biology and The Taub Institute for Research on Alzheimer's Disease and the Aging Brain v; Columbia University, New York, NY 10032

Abstract

Caspases play critical roles in Alzheimer's disease (AD) pathogenesis. Here we show that caspase-2 is required for the cognitive decline seen in hAPP transgenic mice (J20). The age-related changes in behavior and dendritic spine density observed in these mice are absent when they lack caspase-2, in spite of similar levels of A β deposition and inflammation. A similar degree of protection is observed in cultured hippocampal neurons lacking caspase-2, which are immune to the synaptotoxic effects of A β . Our studies suggest that caspase-2 is a critical mediator in the activation of the RhoA/ROCK-II signaling pathway, leading to the collapse of dendritic spines. We propose that this is controlled by an inactive caspase-2/RhoA/ROCK-II complex localized in dendrites, which dissociates in the presence of A β , allowing for their activation and entry in the spine. These findings directly implicate caspase-2 as key driver of synaptic dysfunction in AD and offer novel therapeutic targets.

INTRODUCTION

Mice that carry transgenes encoding mutant human amyloid precursor protein (hAPP) develop many of the changes associated with Alzheimer's disease (AD), including deficits in learning and memory, inhibition of long-term potentiation (LTP), loss of dendritic spines, profuse amyloid plaques and increased phosphorylation of the tau protein¹. Changes similar to those seen in transgenic animals are replicated *in vitro* by treatment of cultured primary neurons with aggregated soluble A β oligomers, or *in vivo* by direct injection of A β oligomers into the hippocampus^{2,3}. Because neuronal death is usually not observed in hAPP transgenic mice, the non-apoptotic role of caspases (cysteine-aspartic proteases), in driving

Users may view, print, copy, download and text and data-mine the content in such documents, for the purposes of academic research, subject always to the full Conditions of use: http://www.nature.com/authors/editorial_policies/license.html#terms

To whom correspondence should be addressed: 630 W. 168th Street, New York, NY 10032, mls7@columbia.edu.

²Present address: Division of Psychological Medicine and Old Age Psychiatry, Institute of Psychiatry; King's College London, De Crespigny Park, Denmark Hill London SE5 8AF

[†]J. Pozueta and R. Lefort contributed equally to this work.

Author Contributions

J.P. and R.L. contributed equally to this work. All authors contributed to the design of the experiments. J.P., R.L. and E.M.R. performed the experiments. J.P., R.L. and M.S. wrote the paper. O.A. analyzed and interpreted the behavioral data. All authors discussed the results and implications and commented on the manuscript at all stages.

The authors declare no competing financial interests.

AD-related changes have remained largely unexplained. However, it is clear that caspases are crucial in contexts other than apoptosis, particularly in the maintenance of normal synaptic functions, whether in sculpting dendritic arborization and synapses^{4,5}, guiding and pruning axons^{6,7}, or in regulating LTP and LTD^{8,9}.

Disruption of normal synaptic function is one of the earliest events in AD^{10,11}, raising the intriguing possibility that aberrant activation of caspases in AD brains may also play a pathogenic non-apoptotic role in driving these synaptic changes. Several caspases have been shown to be activated in human and in AD mouse model brains, including caspase-1, caspase-2, caspase-3, caspase-6 and caspase-9^{12–16}. Of all these caspases however, our work has shown that only caspase-2 appears to be required for the apoptotic effects of A β in cultured hippocampal neurons. Hippocampal neurons for caspase-2 null mice are resistant to A β in spite of elevated levels of caspase-3, caspase-9 and the pro-apoptotic protein Smac/Diablo^{17,18}.

In the current study, we have revisited these earlier findings and investigated whether caspase-2 also plays a significant role in mediating the effects of A β on synaptic plasticity and memory. We approached this question first in the J20 transgenic AD mouse model¹⁹. This mouse model features elevated levels of A β 42, resulting from the introduction of the Swedish (K670N/M671L) and Indiana (V717F) hAPP mutations (i.e. hAPPSwInd) and develop numerous plaques by the age of 5–7 months, as well as an age-dependent decline in learning in memory. We show that crossing the J20 mice with caspase-2 null mice results in the complete prevention of the memory impairments, as assessed by the radial arm water maze, and prevention of the loss of dendritic spine density typically observed in J20 mice, without significantly affecting amyloid load, inflammation and neuritic dystrophy. We further validated these results in an *in vitro* AD model using cultured primary hippocampal neurons where we show that down-regulation of caspase-2 blocks the A β -mediated changes in dendritic spines. Additionally, our data suggest that caspase-2 may be a critical component in the activation and signaling of the Rho-GTPase RhoA, a critical regulator of dendritic spine morphology^{20,21}. Taken together, these studies suggest that caspase-2 plays a critical role in mediating the synaptic changes and memory alteration induced by A β in AD, and highlight caspase-2 as a potential target for AD therapy.

RESULTS

Synaptotoxic effects of A β requires caspase-2

In order to determine if caspase-2 plays a role in the subapoptotic effects of oligomeric A β at low (nM range) concentrations, in addition to its apoptotic role at higher (μ M range) doses (Supplementary Fig. S1a), we exposed hippocampal neurons from wild-type rats to 300 nM A β with and without down-regulation of caspase-2 and examined the effects on dendritic spine density and on levels of RhoA-GTP and ROCK-II. This resulted in a progressive decrease in spine density over the initial 24 hours of exposure as well as increases in the levels of active RhoA-GTP and ROCK-II (Fig. 1a, b and Supplementary Fig. S1b, c). These effects were not seen in neurons exposed to the reverse A β peptide 42-1 (Supplementary Fig. S2). When caspase-2 levels were decreased with an siRNA by 65% (Fig. 1f), there was a partial blockade of the effect of A β on spine density and the levels of RhoA-GTP and

ROCK-II, and complete protection against A β -induced spine reduction (Fig. 1c–e, g). Down-regulation of caspase-3, caspase-8 and caspase-9 individually had no effect on spine density or on the levels of RhoA-GTP (Fig. 2a, b, e–g). Since siRNA-mediated down-regulation of each caspases was not complete (Fig. 2f), we wanted to rule out the possibility that residual caspase activity was responsible for the lack of protection. For that, we used commercially available irreversible caspase inhibitors to block caspase activity. Consistent with our siRNA results, only the caspase-2 inhibitor (VDVAD) blocked the effects of A β on dendritic spines, while the caspase-3 (DEVD) and caspase-8 (LEHD) inhibitors had no significant protective effect (Fig. 2c, d). These results were confirmed using hippocampal neurons from wild-type (WT) and caspase-2 null mice (Casp2KO). Prior to A β treatment, the spine density in neurons from each mouse line was similar. However, when the neurons were treated with A β , a significant loss of spines (~50% after 24h) was seen in WT neurons but not in those derived from the Casp2KO mice (Fig. 1h). These experiments suggest that caspase-2 is not only critical for A β -induced apoptosis but also for the effects of A β on dendritic spines in cultured neurons.

Memory impairments are absent in J20 mice lacking caspase-2

Since experiments in cell culture are acute and cannot provide data on chronic effects or on the relationship of these changes to alterations in memory, we generated a new transgenic mouse line by crossing J20 mice¹⁹ that overexpress mutant hAPP carrying the Swedish (K670N/M671L) and Indiana (V717F) hAPP mutations (i.e. hAPPSwInd), with caspase-2 knock-out (Casp2KO) mice²², with both parental lines being on C57BL/6 backgrounds. Four distinct lines with four different genotypes were derived from these crosses: hAPP^{-/-}/Casp2^{+/+} referred to as wild-type (WT); hAPP^{+/-}/Casp2^{+/+} referred to as J20; hAPP^{+/-}/Casp2^{-/-} referred to as J20/Casp2KO and hAPP^{-/-}/Casp2^{-/-} referred to as Casp2KO. We analyzed these mice for dendritic spine morphology, amyloid accumulation, astrocytosis, microgliosis, dystrophic neurites and behavior, as measured by radial arm water maze.

The animals were tested in the radial arm water maze (RAWM) at 4 months, 9 months and 14 months of age and then sacrificed. The brains were examined by diOlistic labeling to determine dendritic spine density and the levels of active RhoA-GTP and ROCK-II were measured by Western blotting. Since differences in behavior or in dendritic spine density could simply reflect differences in A β load or deposition, sections were also stained for plaques with an A β specific antibody (6E10), and levels of soluble and acid-extractable A β were measured at each of the ages. Since the results at 9 and 14 months were quite similar, we will focus our discussion on the changes at 14 months.

At 4 months of age there were no detectable amyloid plaques in the brains of any of the 4 mouse lines and extractable A β levels showed no significant differences. No significant difference in task acquisition in RAWM was seen among the lines at 4 or 9 months of age (Fig. 3a, b). On the contrary, at 14 months of age the J20 animals and the Casp2KO animals were slower to learn the task than either WT or J20/Casp2KO animals (Fig. 3c). More importantly, only the J20 animals were impaired in task retention when compared to the three other lines at 4, 9 and 14 months of age (Fig. 3d–f). The differences in task retention were independent of motor, sensory or motivational changes among the different lines, as

there were no observable changes in the latency to find a visible platform or in the swimming speed of these mice (Figure 3g, h).

Synaptic changes are abrogated in J20 mice lacking caspase-2

Immediately after the behavioral analyses described above, the mice were sacrificed to evaluate whether the differences in behavior were reflected by changes in dendritic spine density and morphology. Spine density did not differ greatly at 4 months of age among genotypes (Fig. 4a). Moreover, there were no significant alterations in PSD95, Synapsin-1, RhoA-GTP or ROCK-II at 4 months of age (Supplementary Fig. S3a, b). However, analysis of spine morphology at this age revealed a significant decrease in the mushroom subtype in the J20 mice as compared with the WT and the J20/Casp2KO mice. The decrease in mushroom spines in the J20 animals is correlated with an increase in the stubby subtype that was not seen in the other lines (Fig. 4c–e). When similar studies were carried out at 14 months of age, dendritic spine density in the J20 animals was reduced to approximately 50% of the level seen in WT animals while the J20/Casp2KO animals, and the Casp2KO animals showed no loss of dendritic spines (Fig. 4a, b). To determine if these changes were limited to the hippocampus, we examined the frontal cortex where we found similar spine changes (Supplementary Fig. S3c). Similarly, biochemical analysis of the hippocampus at 14 months showed a reduction in both PSD95 and Synapsin-1 and an increase in RhoA-GTP and ROCK-II in the J20 animals (Fig. 4f, g). No changes in these markers were seen in the other three lines.

At 14 months of age, both the J20 and J20/Casp2KO animals showed approximately equal accumulation of amyloid plaques (Fig. 5a, b) and equal levels of expression of hAPP (Fig. 5d). No plaques were seen in the WT and Casp2KO animals and no hAPP expression was found. Levels of soluble and formic acid-extractable A β did not differ significantly between J20 and J20/Casp2KO mice (Fig. 5e). While differences did not meet statistical significance, A β levels appeared be marginally lower in the J20/Casp2KO animals. GFAP staining revealed similar increases in astrogliosis both in the J20 and J20/Casp2KO as compared with the WT and Casp2KO animals (Fig. 5a, c). Increased tau phosphorylation is seen in the J20 animals but not in the J20/Casp2KO animals (Supplementary Fig. S3d). Staining for dystrophic neurites with SMI-312^{23,24} and for microglia with Iba-1²⁵ showed no significant difference between the J20 and J20/Casp2KO mice in the area surrounding the amyloid plaques (Supplementary Fig. S4a–c).

Caspase-2 and inactive RhoA form a complex

It has been demonstrated that A β -treatment of neurons activates caspase-2²⁶. The results presented above suggest that caspase-2 might play a role in the regulation of dendritic spine dynamics through RhoA. It has been reported that RhoB, a protein that is over 90% homologous with RhoA, is capable of binding to caspase-2²⁷. To determine if a similar interaction underlies the role of caspase-2 in A β -mediated synaptic changes, we examined the interaction of these proteins in a series of co-immunoprecipitation (coIP) studies from lysates of primary hippocampal neurons. We found that inactive RhoA (RhoA-GDP) but not active RhoA (RhoA-GTP) co-precipitated with caspase-2 (Fig 6a). We were unable to directly immunoprecipitate RhoA-GDP or RhoA-GTP with the antibodies at our disposal

and therefore turned to a cell-free system using recombinant caspase-2 and recombinant His-tagged inactive RhoA [His-RhoA] and His-tagged constitutively active RhoA [His-RhoA(Q63L)]. Consistent with our *in vitro* coIP studies, only His-RhoA co-precipitated with caspase-2, but not constitutively active RhoA [His-RhoA(Q63L)]. Conversely, caspase-2 co-precipitated only with inactive His-RhoA, and not with active His-RhoA(Q63L) (Fig. 6b, c). Together, these results suggest a direct interaction between caspase-2 and inactive RhoA and not with active RhoA. This interaction does not appear to inhibit the activity of caspase-2, since the addition of inactive RhoA to recombinant active caspase-2 failed to block its activity as measured by fluorometric assay (Supplementary Fig. S5a).

Synaptotoxic effects of A β are RhoA/ROCK-II dependent

Interestingly, we found that the activity of caspase-2 may be critical in mediating the effects of A β on cytoskeletal dynamics through its recently reported role in cleaving and activating the RhoA effector ROCK-II²⁸. Indeed, exposure of primary hippocampal neurons to A β resulted in increased ROCK-II cleavage, generating a ~130kDa fragment (Supplementary Fig. S6a, b), consistent with previous reports^{28,29}. Depletion of caspase-2 in these neurons prior to A β treatment blocked ROCK-II cleavage, confirming the role of caspase-2 in cleaving ROCK-II.

If RhoA and ROCK-II play critical roles in A β -mediated dendritic spine alterations, we would predict that inhibition of their activities should be able to block these changes. When primary hippocampal neuronal cultures were pretreated with the RhoA inhibitor, C3 transferase, or the ROCK-II inhibitor, Y27632, and then exposed to A β , the changes in spine density were abrogated (Fig. 6d, e). To determine if caspase-2 was involved more broadly in the control of RhoA mediated signaling. We treated cells for 1h with lysophosphatidic acid (LPA) leading to the large increase in RhoA-GTP. Pretreatment of the cells with either siCasp2 or the commercially available caspase-2 inhibitor VDVAD partially blocks the increase in RhoA-GTP suggesting that caspase-2 is involved in regulating RhoA in response to diverse stimuli (Supplementary Fig. S5b, c).

Caspase-2 regulates RhoA localization

There is evidence that suggests that the distribution of RhoA may be altered in AD and in AD mouse models³⁰. We wondered whether A β could affect the localization of RhoA in neurons and whether caspase-2 plays a role in this process. We exposed primary hippocampal neurons to A β and measured the localization of PSD95, RhoA and caspase-2 over the course of 24 hours. (Fig. 7a, b, f, g). Prior to treatment with A β we found very low levels (~10%) of colocalization of RhoA with the synaptic marker PSD95 (Figure 7a, c), suggesting that the majority of RhoA is found outside dendritic spines. After treatment with A β , there was a significant increase (~20%) after 6 hours in the co-localization of RhoA and ROCK-II with PSD95, suggesting that A β treatment results in the recruitment of these proteins to dendritic spines, a translocation that has been suggested for RhoA in response to glutamate receptor modulation³¹. While the ROCK-II increase at the spine is significant by 1h and remains elevated over the treatment period the RhoA translocation is more gradual. Similarly, prior to treatment, caspase-2 was mostly present in the dendritic shaft (Figure 7a,

f), but after treatment with A β , we observed a clear increase (~10%) in caspase-2 colocalization with PSD95 between 1h and 6h post-treatment (Figure 7d), suggesting that A β also triggers the translocation of caspase-2 to dendritic spines. When caspase-2 was down-regulated in neurons prior to treatment with A β , the colocalization of RhoA and PSD95 was significantly diminished (Figure 7f, g), consistent with a role for caspase-2 as a facilitator of RhoA translocation to dendritic spines after A β treatment. A β treatment also resulted in increased co-localization of caspase-2 with both RhoA and ROCK-II consistent with an interaction between caspase-2 and these proteins (Fig. 7e, i). Down-regulation of caspase-2 prior to A β treatment significantly reduced the translocation of both RhoA and ROCK-II to the spines (Fig. 8).

Taken together, these results suggest that caspase-2 exerts at least a portion of its effects by controlling the localization, and perhaps the activity of the RhoA/ROCK-II signaling pathway leading to modulation of the actin cytoskeleton in the dendritic spines.

DISCUSSION

Caspases have are most often thought of in connection with apoptosis. However, several lines of evidence have shown that caspases can also mediate a series of regulatory events in the mature nervous system designed to refine neuronal circuits, such as axon pruning and synapse elimination⁴⁻⁷. These processes are tightly regulated presumably by restricting the duration and location of caspase activation³². This implies that aberrant and mislocalized activation of caspases in living neurons could have detrimental effects on normal physiology and synaptic functions. Indeed, a number of caspases have been implicated in neurodegenerative diseases, including AD¹²⁻¹⁶. We previously demonstrated that caspase-2 was required, with caspase-3 being dispensable, for the apoptosis-inducing effects of A β in cultured hippocampal neurons^{17,18}. Naturally, this led us to wonder whether caspase-2 was also involved in the synaptotoxic effects of A β .

Using genetic, reverse genetic and pharmacologic tools, both in primary neuronal culture and in the intact animal, we show that caspase-2 is the key regulator of dendritic spine density and morphology in response to A β . We found that knocking out caspase-2 in the J20 mice, completely prevented many of the age-dependent AD-like changes, including the memory deficits in performing the radial arm water maze and the increase in phosphorylated tau protein (pTau). Knocking out caspase-2 in these mice completely abrogated the changes in spine morphology at an early age (4 months) and blocked the loss of dendritic spine density in older mice (14 months).

It is interesting to note that the protective effects of knocking out caspase-2 in these animals occur without any significant changes in the levels of soluble A β or in the extent of plaque load. This raises an intriguing question as to whether AD-like changes in these animal models are due to A β or to overexpression of APP. The fact that these animals improve without much change to the A β burden suggests the possibility that much of the pathology is A β -independent. However, this oversimplifies the intimate relationship between A β and APP signaling. For example, while A β has been demonstrated to be highly toxic to cultured neurons³³, APP itself appears to be necessary for this toxicity to occur³⁴. The induction of

APP signaling by its dimerization may in fact be sufficient to trigger neuronal death³⁵. However, APP dimerization also leads to increased A β production^{36–38} and to the formation of an APP-derived cytosolic toxic fragment, C31^{39–41}. Interestingly, blocking the formation of C31 also causes the reversal of cognitive impairments in J20 mice without affecting the levels of A β ^{42,43}. In our cell culture experiments it is clear that A β causes changes similar to those seen in the mouse and the transduction of these signals requires APP cleavage^{39–41}.

In aggregate, these findings suggest a complex interrelation between accumulating A β and signaling by APP, its soluble APP ectodomains and its intracellular C-terminal fragments in mediating AD-like changes in animal models. Reducing the levels of any of these components eventually halts this complex signaling machinery allowing for the reversal of the associated cognitive decline⁴⁴. The relative importance of elements of this pathway may differ with the stage of the disease and may explain the failure therapeutic strategies designed solely to decrease the levels of A β .

The protective effects of knocking out caspase-2 were also recapitulated in a cellular model of AD-related synaptic dysfunction. Both siRNA and chemical inhibitor-mediated approaches to silence or inhibit caspase-2 proved successful in blocking the synaptotoxic effects of A β in cultured hippocampal neurons. Consistent with our previous report, silencing of caspase-3, caspase-8 and caspase-9 individually could not protect cultured neurons against A β exposure. Taken together, these results suggest that caspase-2 is a key player in a novel mechanism regulating dendritic spine architecture and neural function that is ultimately mirrored in the behavioral tasks.

These results are at variance with two recent reports implicating caspase-3 in the modulation of spine dynamics in similar mouse models^{45,46}. It should be noted that the first of these studies relied on the detection of cleaved caspase-3 as a measure of activity. However, the cleavage of caspase-3 does not necessarily indicate that it is active in cells. Indeed caspases are subject to regulation by a wide array of IAPs (inhibitor of apoptosis) and other regulatory proteins^{18,47}. In the absence of specific intracellular reporters, *in situ* bVAD trapping of active caspases⁴⁸ remains the most reliable way to confirm that a given caspase is active. Furthermore, the exclusive reliance on pseudosubstrate inhibitors in that study precludes drawing any definitive conclusion as to the involvement of a specific caspase, since these inhibitors lack the required specificity⁴⁹. The second report attempts to overcome several of these limitations by using the BIR domain of IAP proteins to specifically block caspase-3 activity. While this domain does not affect caspase-2 activity, the analysis of the data is confounded by the fact that the BIR domain can also directly interact with cytoskeletal elements and block cytokinesis, as demonstrated in *C. elegans*⁵⁰. Furthermore, the XIAP ring domain can also interact with Rho-regulatory protein, RhoGDI and promote the assembly of actin, a key component of dendritic spines⁵¹. Thus, it cannot be ruled out that the BIR-mediated protective effect is due to action on the actin cytoskeleton rather than on inhibition of caspase-3. The fact that depleting the protein levels of caspase-3 through RNAi in our studies fails to confer any protection against A β in neurons argues against a central role for caspase-3 in this process.

The exact mechanism by which caspase-2 mediates the synaptotoxic effects of A β is an intriguing one and our results offer several important clues. Both caspase-2 and RhoA appear to reside outside of the spine head in the form of an inactive complex under normal conditions. This is supported by the fact that only inactive RhoA co-precipitates with caspase-2 and by the fact that we observe very little colocalization between them and the synaptic marker, PSD95. However, exposure to A β results in the activation of both caspase-2 and RhoA and the dissociation of the complex (Figure 9). In their active form, both RhoA and caspase-2 appear to enter the spine head, demonstrated by the fact that there is a significant increase in their co-localization with PSD95. One interesting observation is that down-regulating caspase-2 is not sufficient for the translocation of RhoA to spines, suggesting that another anchor may be preventing this occurrence. A possible candidate for this role is the Rho-GDP dissociation inhibitor (RhoGDI), which sequesters Rho-GTPases from the membrane and prevents their interaction with guanine exchange factors (GEFs). An interesting line for future investigations is to determine if both caspase-2 and Rho-GDI complex with RhoA-GDP at the same time or whether their binding is mutually exclusive.

Once active RhoA and caspase-2 enter the spine head, they can affect the activity of one or more effectors to drive the collapse of the spines. One immediate candidate is the Rho effector ROCK-II, which has previously been shown to be activated by caspase-2 mediated cleavage²⁸, and which we show to be cleaved in neurons treated with A β .

In summary, our results clearly demonstrate that caspase-2 is an important mediator of A β synaptotoxicity in culture and in the intact animal. Since caspase-2 expression is elevated in AD brain^{52,53}, it is possible that inhibition of caspase-2, especially early in the course of AD, might prevent synaptic changes and memory deficits. The fact that we can protect neurons against A β with only a partial down-regulation of caspase-2 suggests that therapeutic protection might be achieved without blocking critical actions of caspase-2 in other systems.

METHODS

Transgenic mice

All animal studies were performed according to protocols examined and approved by the Animal Use and Care Committee of Columbia University. The J20 transgenic mouse line expresses a mutated human APP (hAPP: K670N/M671L and V717F) under the control of the platelet-derived growth factor promoter^{19,54}. In our studies we have used a J20 mouse line crossed to a C57BL/6 background (courtesy of Dr. S-D Yan). Caspase-2 knockout (Casp2KO) mice²² were also back-crossed to a C57BL/6 background. Double transgenic mice were obtained by crossing hemizygous transgenic mice J20 with Casp2KO mice. The first generation was crossed again with Casp2KO mice to generate the dual transgenic/null J20/Casp2KO mice. Transgenic mice were genotyped by PCR using oligonucleotides for human APP and caspase-2 with PuRe Taq PCR beads (Amersham).

Male mice were divided into the following groups: wild-type (WT), caspase-2 knockout (Casp2KO), J20 and J20/Casp2KO. Mice were tested blindly in the following experimental sequence: behavior, biochemistry, and histology. The complete sequence of behavioral tests

was performed in the same mice at 4, 9 and 14 months of age. For each of the age groups, the complete sequence of behavioral tests required approximately 3 weeks and consisted of the radial-arm water maze (RAWM) test, and visible platform test. Immediately after behavioral testing at 14 month of age, mice were killed for DiOlistic labeling, biochemical, and histological studies. Female mice were used only for the DiOlistic labeling, the biochemical, and histological studies and not for the behavioral studies.

Radial-arm water maze

The task has been described previously⁵⁵. Each day of testing included 4 consecutive trials (A1–A4) and a fifth trial (R) 30 minutes after the fourth trial. The first 4 trials tested acquisition of the task, while the fifth trial tested retention memory (short-term memory). Each trial lasted 1 minute. Errors were counted when the mouse went to an arm without platform or took more than 20 seconds to enter any arm of the maze. The number of errors in each trial in the last 3 days of testing was averaged and used for statistical analysis.

DiOlistic labeling

DiOlistic labeling was performed as previously described⁵⁶. Briefly, mice were anesthetized then fixed with 4% paraformaldehyde (PFA) by transcardiac perfusion. Their brains were removed and sectioned coronally (300 μ M) using a vibratome. Tissue sections were subsequently shot with DiI-coated particles using the Helios gene gun system. Hippocampal neurons were visualized using a spinning Disk Confocal Microscope and images were acquired with Perkin Elmer Volocity Software. Spines were counted manually in a double-blinded manner. NeuronStudio software was used to analyze the spine subtype populations.

Histological studies

Immunolabeling was done on 30 μ m brain sections from the four genotypes. Staining was done using the anti A β antibody 6E10 (Covance), A β _{1–42} (Abbiotech), Pan-Axonal Neurofilament SMI-312 (Covance), GFAP (Cell Signaling), anti microglia Iba-1 (Abcam). Plaque load and astrocytosis were quantified using ImageJ. Total plaque area was expressed as a percentage of the total hippocampal area. Astrocytosis was expressed as total area units.

ELISA and Western blot analysis

Whole frozen hippocampi were homogenized using a Teflon dounce homogenizer first in 150 mg/ml in 2% w/v sodium dodecyl sulfate (SDS) in water with protease inhibitors (Roche) to recover soluble amyloid. The sample was then centrifuged and the pellet homogenized in 70% formic acid in water to obtain the insoluble amyloid fraction. Homogenates were spun at 100,000 \times g for 1 h. Supernates were diluted in buffer EC (0.02 M sodium phosphate, pH 7.0, 0.2 mM EDTA, 0.4 M NaCl, 0.2% bovine serum albumin (BSA), 0.05% CHAPS) on ice. To obtain the soluble amyloid fraction and protein for Western blotting, frozen hippocampi were homogenized using a Teflon dounce homogenizer in cell lysis buffer (Cell Signaling), sonicated briefly and centrifuged at 14,000 rpm for 10 min. A β _{X-42} was measured by ELISA (Covance) following the manufacturers protocol. Immunoblotting was performed using the following polyclonal antibodies C-terminal APP

(Calbiochem), caspase-2 (Ab-cam), PSD95 (Cell Signaling), Synapsin-1 (Chemicon) and ERK1 (Santa Cruz) and the monoclonal antibody for phospho-tau PHF13 (Cell Signaling). The caspase-2 polyclonal antibody was provided by the Troy laboratory⁵⁷. Representative complete gels can be found in the Supplementary Information (Supplementary Figure S7).

Immunofluorescence and microscopy

Cells were fixed in PFA (4%) in PBS for 10 min. Permeabilization was performed using 0.4% triton in PBS for 20 min. Cells were stained using the following antibodies PSD95 (Cell Signaling), Syn-apsin-1 (Chemicon) and caspase-2 (Millipore). Primary cultures were visualized using a spinning disk confocal microscope and images were acquired with Perkin Elmer Volocity software.

Data analysis and statistics

Immunoblotting, primary cultures spine density, behavioral, ELISA analysis, and plaque burden analyses were performed with a two-tailed Student *t* test. Mouse spine density data were analyzed by two-way ANOVA with age and genotype as independent variables. In all cases, $P < 0.05$ was considered to be statistically significant.

Supplementary Material

Refer to Web version on PubMed Central for supplementary material.

Acknowledgments

This work was supported in part by grants NIHAG08702, the Wallace Foundation for Research and the Taub Foundation.

References

1. McGowan E, Eriksen J, Hutton M. A decade of modeling Alzheimer's disease in transgenic mice. *Trends in genetics : TIG*. 2006; 22:281–289. [PubMed: 16567017]
2. McLarnon JG, Ryu JK. Relevance of abeta1–42 intrahippocampal injection as an animal model of inflamed Alzheimer's disease brain. *Curr Alzheimer Res*. 2008; 5:475–480. [PubMed: 18855589]
3. Vitolo O, et al. Protection against beta-amyloid induced abnormal synaptic function and cell death by Ginkgolide J. *Neurobiol Aging*. 2009; 30:257–265. [PubMed: 17640772]
4. Kuo CT, Zhu S, Younger S, Jan LY, Jan YN. Identification of E2/E3 ubiquitinating enzymes and caspase activity regulating *Drosophila* sensory neuron dendrite pruning. *Neuron*. 2006; 51:283–290. [PubMed: 16880123]
5. Williams DW, Kondo S, Krzyzanowska A, Hiromi Y, Truman JW. Local caspase activity directs engulfment of dendrites during pruning. *Nat Neurosci*. 2006; 9:1234–1236. [PubMed: 16980964]
6. Nikolaev A, McLaughlin T, O'Leary DD, Tessier-Lavigne M. APP binds DR6 to trigger axon pruning and neuron death via distinct caspases. *Nature*. 2009; 457:981–989. [PubMed: 19225519]
7. Ohsawa S, et al. Maturation of the olfactory sensory neurons by Apaf-1/caspase-9-mediated caspase activity. *Proc Natl Acad Sci U S A*. 2010; 107:13366–13371. [PubMed: 20624980]
8. Li Z, et al. Caspase-3 activation via mitochondria is required for long-term depression and AMPA receptor internalization. *Cell*. 2010; 141:859–871. [PubMed: 20510932]
9. Jiao S, Li Z. Nonapoptotic function of BAD and BAX in long-term depression of synaptic transmission. *Neuron*. 2011; 70:758–772. [PubMed: 21609830]
10. Masliah E, et al. Synaptic and neuritic alterations during the progression of Alzheimer's disease. *Neurosci Lett*. 1994; 174:67–72. [PubMed: 7970158]

11. Ingelsson M, et al. Early Abeta accumulation and progressive synaptic loss, gliosis, and tangle formation in AD brain. *Neurology*. 2004; 62:925–931. [PubMed: 15037694]
12. Allen JW, Eldadah BA, Huang X, Knoblach SM, Faden AI. Multiple caspases are involved in beta-amyloid-induced neuronal apoptosis. *J Neurosci Res*. 2001; 65:45–53. [PubMed: 11433428]
13. Sheng JG, et al. Neuronal DNA damage correlates with overexpression of interleukin-1beta converting enzyme in APPV717F mice. *Neurobiol Aging*. 2001; 22:895–902. [PubMed: 11754996]
14. Pellegrini L, Passer BJ, Tabaton M, Ganjei JK, D'Adamio L. Alternative, non-secretase processing of Alzheimer's beta-amyloid precursor protein during apoptosis by caspase-6 and -8. *J Biol Chem*. 1999; 274:21011–21016. [PubMed: 10409650]
15. LeBlanc A, Liu H, Goodyer C, Bergeron C, Hammond J. Caspase-6 role in apoptosis of human neurons, amyloidogenesis, and Alzheimer's disease. *J Biol Chem*. 1999; 274:23426–23436. [PubMed: 10438520]
16. Guo H, et al. Active caspase-6 and caspase-6-cleaved tau in neuropil threads, neuritic plaques, and neurofibrillary tangles of Alzheimer's disease. *Am J Pathol*. 2004; 165:523–531. [PubMed: 15277226]
17. Troy CM, et al. Caspase-2 mediates neuronal cell death induced by beta-amyloid. *J Neurosci*. 2000; 20:1386–1392. [PubMed: 10662829]
18. Troy CM, et al. Death in the balance: alternative participation of the caspase-2 and -9 pathways in neuronal death induced by nerve growth factor deprivation. *J Neurosci*. 2001; 21:5007–5016. [PubMed: 11438576]
19. Mucke L, et al. High-level neuronal expression of abeta 1–42 in wild-type human amyloid protein precursor transgenic mice: synaptotoxicity without plaque formation. *J Neurosci*. 2000; 20:4050–4058. [PubMed: 10818140]
20. Tashiro A, Yuste R. Regulation of dendritic spine motility and stability by Rac1 and Rho kinase: evidence for two forms of spine motility. *Mol Cell Neurosci*. 2004; 26:429–440. [PubMed: 15234347]
21. Tashiro A, Minden A, Yuste R. Regulation of dendritic spine morphology by the rho family of small GTPases: antagonistic roles of Rac and Rho. *Cereb Cortex*. 2000; 10:927–938. [PubMed: 11007543]
22. Bergeron L, et al. Defects in regulation of apoptosis in caspase-2-deficient mice. *Genes Dev*. 1998; 12:1304–1314. [PubMed: 9573047]
23. Masliah E, Mallory M, Hansen L, DeTeresa R, Terry RD. Quantitative synaptic alterations in the human neocortex during normal aging. *Neurology*. 1993; 43:192–197. [PubMed: 8423884]
24. Masliah E, et al. Comparison of neurodegenerative pathology in transgenic mice overexpressing V717F beta-amyloid precursor protein and Alzheimer's disease. *J Neurosci*. 1996; 16:5795–5811. [PubMed: 8795633]
25. Grathwohl SA, et al. Formation and maintenance of Alzheimer's disease beta-amyloid plaques in the absence of microglia. *Nat Neurosci*. 2009; 12:1361–1363. [PubMed: 19838177]
26. Tizon B, Ribe EM, Mi W, Troy CM, Levy E. Cystatin C protects neuronal cells from amyloid-beta-induced toxicity. *J Alzheimers Dis*. 2010; 19:885–894. [PubMed: 20157244]
27. Kong JY, Rabkin SW. The association between RhoB and caspase-2: changes with lovastatin-induced apoptosis. *Biochemistry and cell biology = Biochimie et biologie cellulaire*. 2005; 83:608–619. [PubMed: 16234849]
28. Sapet C, et al. Thrombin-induced endothelial microparticle generation: identification of a novel pathway involving ROCK-II activation by caspase-2. *Blood*. 2006; 108:1868–1876. [PubMed: 16720831]
29. Sebbagh M, Hamelin J, Bertoglio J, Solary E, Breard J. Direct cleavage of ROCK II by granzyme B induces target cell membrane blebbing in a caspase-independent manner. *The Journal of experimental medicine*. 2005; 201:465–471. [PubMed: 15699075]
30. Huesa G, et al. Altered distribution of RhoA in Alzheimer's disease and AbetaPP overexpressing mice. *J Alzheimers Dis*. 2010; 19:37–56. [PubMed: 20061625]

31. Schubert V, Da Silva JS, Dotti CG. Localized recruitment and activation of RhoA underlies dendritic spine morphology in a glutamate receptor-dependent manner. *J Cell Biol.* 2006; 172:453–467. [PubMed: 16449195]
32. Hyman BT. Caspase activation without apoptosis: insight into Abeta initiation of neurodegeneration. *Nat Neurosci.* 2011; 14:5–6. [PubMed: 21187847]
33. Cavallucci V, D'Amelio M, Cecconi F. Abeta toxicity in Alzheimer's disease. *Mol Neurobiol.* 2012; 45:366–378.10.1007/s12035-012-8251-3 [PubMed: 22415442]
34. Shaked GM, et al. Abeta induces cell death by direct interaction with its cognate extracellular domain on APP (APP 597–624). *FASEB J.* 2006; 20:1254–1256. [PubMed: 16636103]
35. Rohn T, Ivins K, Bahr B, Cotman C, Cribbs D. A monoclonal antibody to amyloid precursor protein induces neuronal apoptosis. *J Neurochem.* 2000; 74:2331–2342. [PubMed: 10820193]
36. Lefort R, Pozueta J, Shelanski M. Cross-linking of cell surface amyloid precursor protein leads to increased beta-amyloid peptide production in hippocampal neurons: implications for Alzheimer's disease. *J Neurosci.* 2012; 32:10674–10685. [PubMed: 22855816]
37. Scheuermann S, et al. Homodimerization of amyloid precursor protein and its implication in the amyloidogenic pathway of Alzheimer's disease. *The Journal of biological chemistry.* 2001; 276:33923–33929. [PubMed: 11438549]
38. Munter LM, et al. GxxxG motifs within the amyloid precursor protein transmembrane sequence are critical for the etiology of Abeta42. *EMBO J.* 2007; 26:1702–1712. [PubMed: 17332749]
39. Lu DC, et al. A second cytotoxic proteolytic peptide derived from amyloid beta-protein precursor. *Nat Med.* 2000; 6:397–404. [PubMed: 10742146]
40. Lu DC, Shaked GM, Masliah E, Bredesen DE, Koo EH. Amyloid beta protein toxicity mediated by the formation of amyloid-beta protein precursor complexes. *Ann Neurol.* 2003; 54:781–789. [PubMed: 14681887]
41. Lu DC, Soriano S, Bredesen DE, Koo EH. Caspase cleavage of the amyloid precursor protein modulates amyloid beta-protein toxicity. *J Neurochem.* 2003; 87:733–741. [PubMed: 14535955]
42. Galvan V, et al. Reversal of Alzheimer's-like pathology and behavior in human APP transgenic mice by mutation of Asp664. *Proc Natl Acad Sci USA.* 2006; 103:7130–7135. [PubMed: 16641106]
43. Saganich MJ, et al. Deficits in synaptic transmission and learning in amyloid precursor protein (APP) transgenic mice require C-terminal cleavage of APP. *J Neurosci.* 2006; 26:13428–13436. [PubMed: 17192425]
44. Melnikova T, et al. Reversible pathologic and cognitive phenotypes in an inducible model of Alzheimer-amyloidosis. *J Neurosci.* 2013; 33:3765–3779. [PubMed: 23447589]
45. D'Amelio M, et al. Caspase-3 triggers early synaptic dysfunction in a mouse model of Alzheimer's disease. *Nat Neurosci.* 2011; 14:69–76. [PubMed: 21151119]
46. Jo J, et al. Abeta(1–42) inhibition of LTP is mediated by a signaling pathway involving caspase-3, Akt1 and GSK-3beta. *Nat Neurosci.* 2011; 14:545–547. [PubMed: 21441921]
47. Troy CM, Shelanski ML. Caspase-2 redux. *Cell Death Differ.* 2003; 10:101–107. [PubMed: 12655298]
48. Tu S, et al. In situ trapping of activated initiator caspases reveals a role for caspase-2 in heat shock-induced apoptosis. *Nat Cell Biol.* 2006; 8:72–77. [PubMed: 16362053]
49. McStay GP, Salvesen GS, Green DR. Overlapping cleavage motif selectivity of caspases: implications for analysis of apoptotic pathways. *Cell Death Differ.* 2008; 15:322–331. [PubMed: 17975551]
50. Fraser AG, James C, Evan GI, Hengartner MO. *Caenorhabditis elegans* inhibitor of apoptosis protein (IAP) homologue BIR-1 plays a conserved role in cytokinesis. *Curr Biol.* 1999; 9:292–301. [PubMed: 10209096]
51. Liu J, et al. X-linked inhibitor of apoptosis protein (XIAP) mediates cancer cell motility via Rho GDP dissociation inhibitor (RhoGDI)-dependent regulation of the cytoskeleton. *J Biol Chem.* 2011; 286:15630–15640. [PubMed: 21402697]
52. Shimohama S, Tanino H, Fujimoto S. Changes in caspase expression in Alzheimer's disease: comparison with development and aging. *Biochem Biophys Res Commun.* 1999; 256:381–384. [PubMed: 10079193]

53. Pompl PN, et al. Caspase gene expression in the brain as a function of the clinical progression of Alzheimer disease. *Arch Neurol.* 2003; 60:369–376. [PubMed: 12633148]
54. Abrahamson E, et al. Caspase inhibition therapy abolishes brain trauma-induced increases in Aβ peptide: implications for clinical outcome. *Exp Neurol.* 2006; 197:437–450. [PubMed: 16300758]
55. Trinchese F, et al. Progressive age-related development of Alzheimer-like pathology in APP/PS1 mice. *Ann Neurol.* 2004; 55:801–814. [PubMed: 15174014]
56. Moolman DL, Vitolo OV, Vonsattel JPG, Shelanski ML. Dendrite and dendritic spine alterations in Alzheimer models. *J Neurocytol.* 2004; 33:377–387. [PubMed: 15475691]
57. Troy C, Stefanis L, Greene L, Shelanski M. Mechanisms of neuronal degeneration: a final common pathway? *Adv Neurol.* 1997; 72:103–111. [PubMed: 8993689]

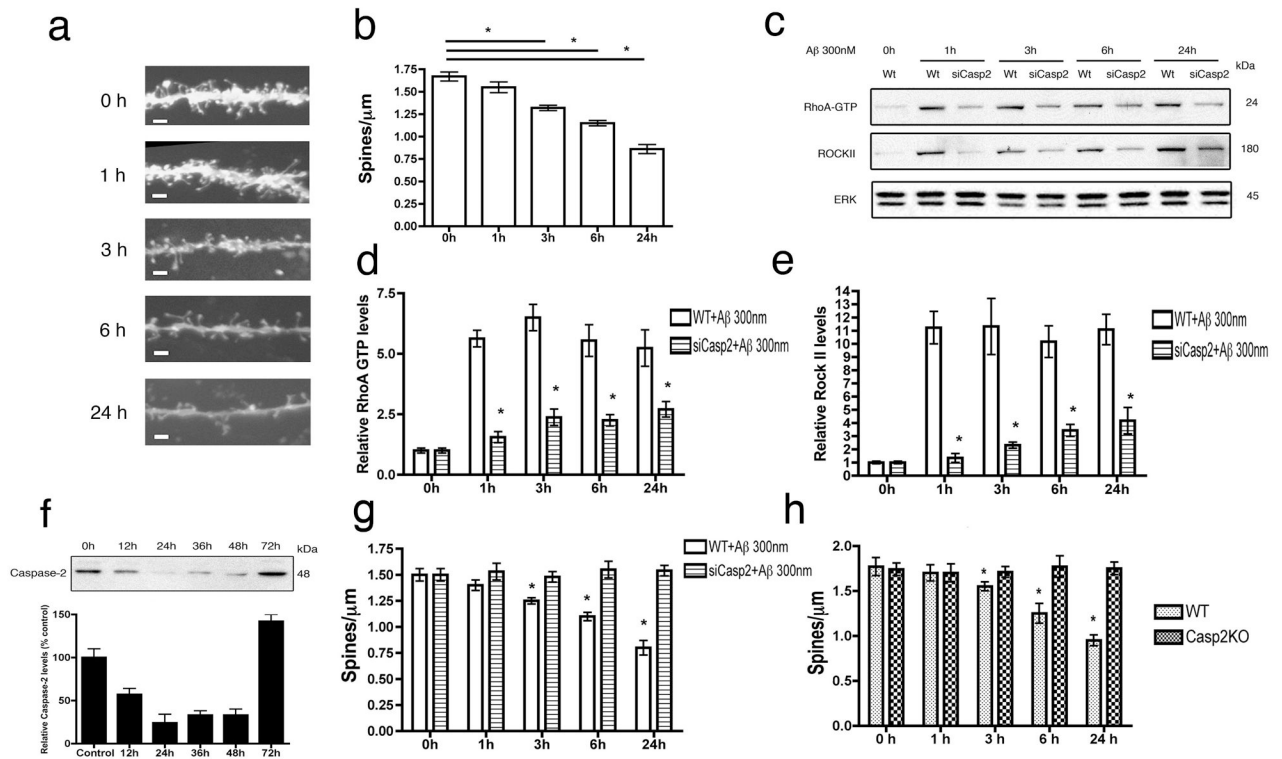


Figure 1. Caspase-2 is required for Aβ induced dendritic spine loss in hippocampal primary cultures

(a) Representative images of labeled dendrites over the course of 24 hours after treatment with 300 nM Aβ. (b) Spine density (spines/μm) changes in rat primary hippocampal cultures treated with 300 nM Aβ for 24h. Data presented as mean ± s.e.m. (n=3 independent experiments, 150 dendrites per point, *p<0.05, one-way ANOVA). (c) Western blot analysis of primary hippocampal cultures pretreated for 12h with 80 nM of Pen1-siRNA against caspase-2 showing no changes in RhoA-GTP or ROCK-II after a 24h treatment with 300 nM Aβ. (d) Densitometric quantification of RhoA-GTP immunoblots. Data presented as the mean ± s.e.m. (n=3 independent experiments, *p<0.05, two-tailed Student's *t*-test). (e) Densitometric quantification of ROCK-II immunoblots. Data presented as the mean ± s.e.m. (n=3 independent experiments, *p<0.05, two-tailed Student's *t*-test). (f) Rat hippocampal primary cultures treated with 80 nM Pen1-siRNA against caspase-2 showing a time-dependent decrease in caspase-2 levels. Representative immunoblot for caspase-2 levels. Densitometric analysis of caspase-2 levels showing a 60% reduction by 12h and persisting over 48h. (g) Rat hippocampal primary cultures pretreated for 24h with 80 nM Pen1-siRNA against caspase-2 show no decrease in spine density after treatment with 300 nM Aβ. Data presented as the mean ± s.e.m. (n=3 independent experiments, 150 dendrites per point, *p<0.05, one-way ANOVA). (h) Hippocampal primary cultures derived from caspase-2 KO mice show resistance to 300 nM Aβ-induced spine loss, while WT neurons are sensitive to treatment. Data presented as the mean ± s.e.m. (n=3 independent experiments, 150 dendrites per point, *p<0.05, one-way ANOVA).

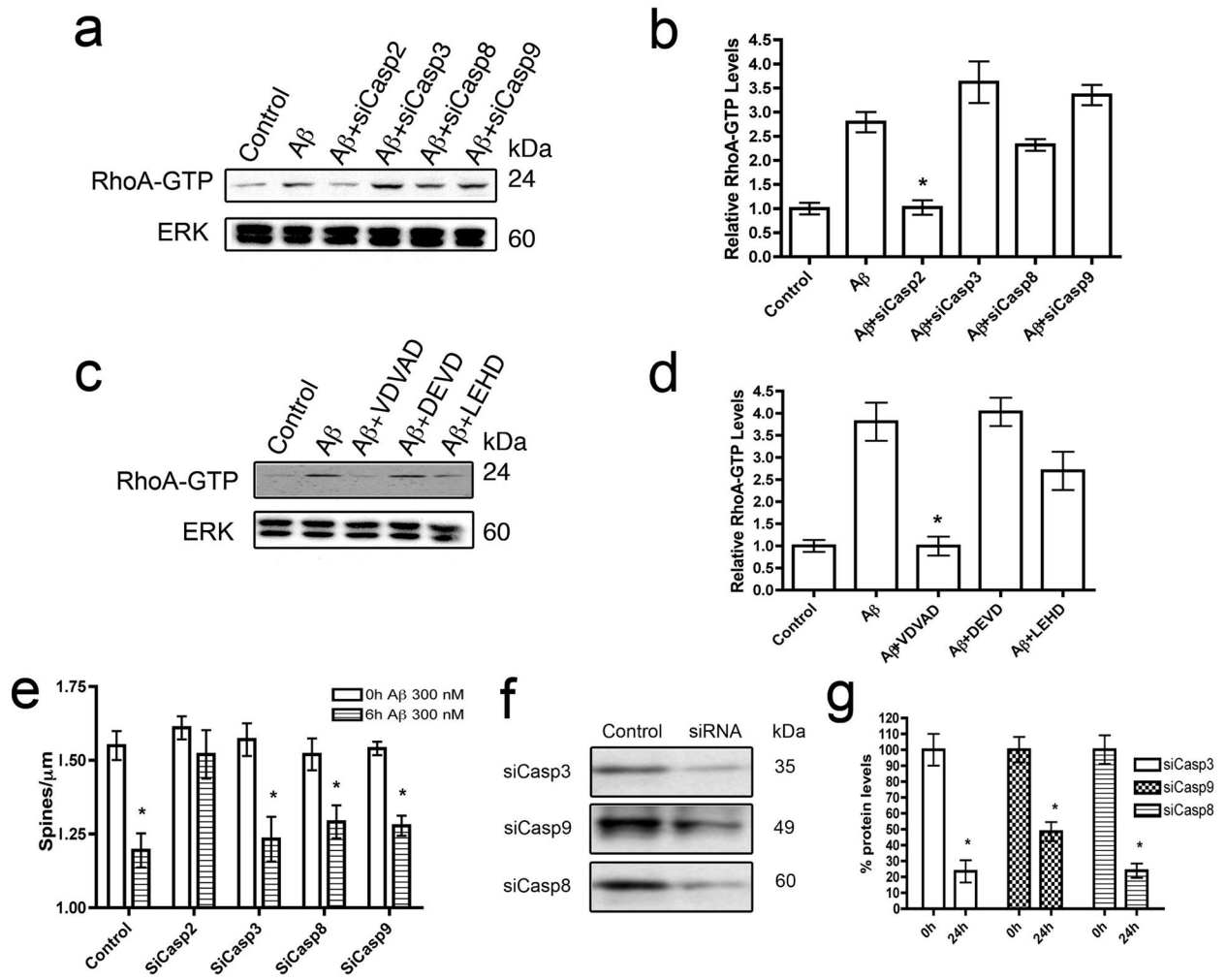


Figure 2. Down-regulation or inactivation of caspase-2 blocks A β -mediated effects on primary hippocampal cultures

(a) Representative Western blot of hippocampal primary cultures treated for 1h with 300 nM A β . The increase in RhoA-GTP levels is reversed by pretreatment with 80nM Pen1-siRNA against caspase-2 but not with siRNA against caspase-3 (siCasp3), -8 (siCasp8) or -9 (siCasp9). (b) Densitometric analysis of RhoA-GTP levels from the immunoblots showing only the siCasp2 is able to block the changes observed from A β . Data presented as the mean \pm s.e.m. (n=3 independent experiments, *p<0.05, two-tailed Student's *t*-test). (c) Representative immunoblot from hippocampal primary cultures treated for 1h with 300 nM A β ; cultures were pretreated for 30 min with 0.5 μ M of each caspase inhibitors: VDVAD (caspase-2); DEVD (caspase-3/7); LEHD (caspase-9). (d) Densitometric representation of RhoA-GTP levels of the immunoblot in panel c. Only caspase-2 inhibitor VDVAD blocks the A β -induced increase in RhoA-GTP. Data presented as the mean \pm s.e.m. (n=3 independent experiments, *p<0.05, two-tailed Student's *t*-test). (e) Spine density in primary hippocampal cultures pretreated for 24h with siRNAs against caspase-2, -3, -8 and -9 and then treated for 6h with 300 nM A β . Only siCasp2 protects against A β -mediated spine changes. Data presented as the mean \pm s.e.m. (n=3 independent experiments, 50 different

dendrites per point; * $p < 0.05$, one-way ANOVA). **(f)** Representative immunoblots of primary cultures treated for 24h with the respective siRNAs. **(g)** Densitometric analysis of caspase-3, -8 and -9 levels after 24h treatment with the siRNA.

Author Manuscript

Author Manuscript

Author Manuscript

Author Manuscript

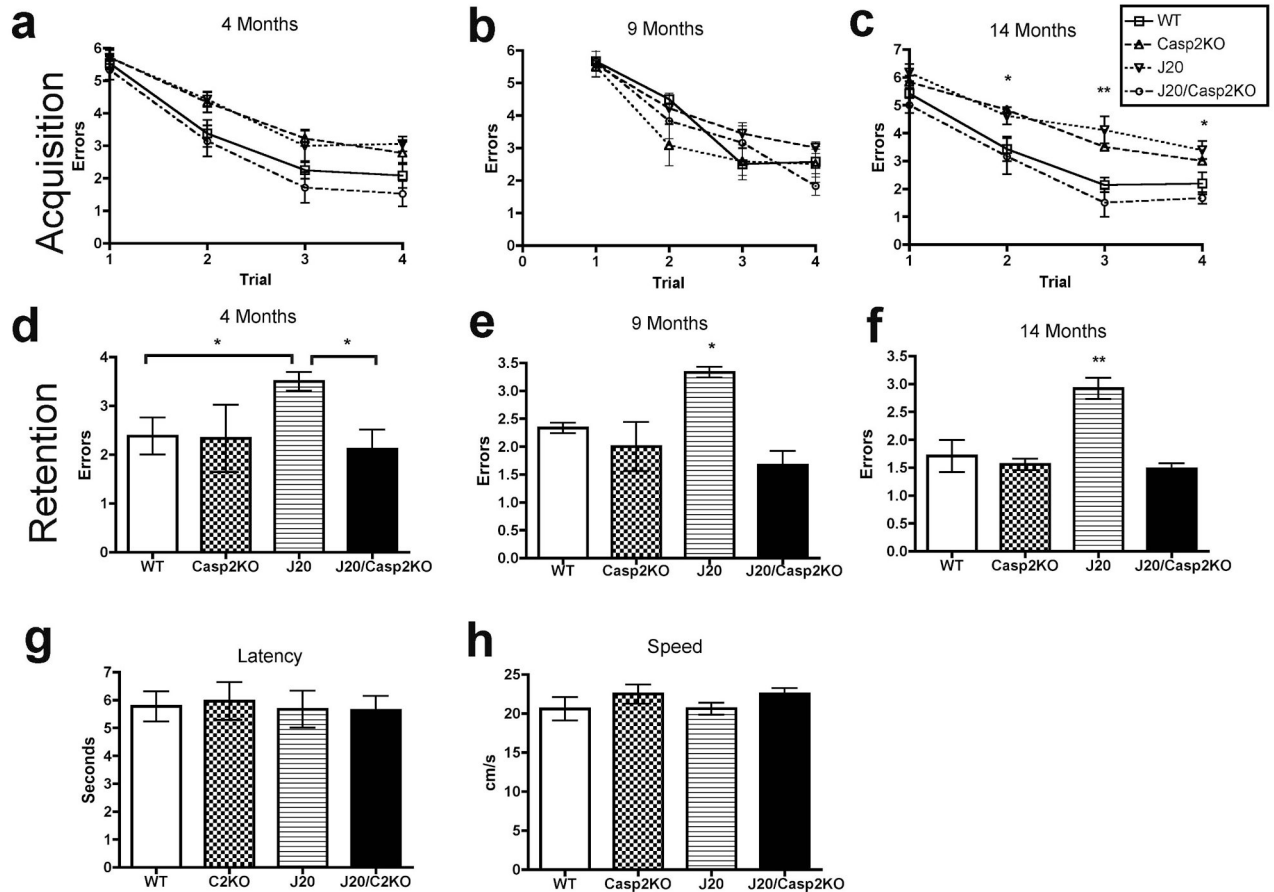


Figure 3. J20/Casp2KO mice lack memory deficits seen in J20 mice

Mice from the four different lines were tested in the radial-arm water maze for spatial working memory at the ages of 4, 9 and 14 months. **(a)** At 4 months, there was no significant difference in task acquisition between WT, Casp2KO, J20 and J20/Casp2KO mice. **(b)** At 9 months, there was no significant difference in task acquisition between WT, Casp2KO, J20 and J20/Casp2KO. **(c)** At 14 months, J20 and Casp2KO mice showed impaired acquisition of the task as compared to WT and J20/Casp2KO littermates (7 male mice per group * $p < 0.05$, two-way ANOVA). **(d)** During the retention trial, 4-month-old J20 mice showed a memory deficit compared with WT and J20/Casp2KO littermates, but not with Casp2KO (7 male mice per group, * $p < 0.05$, two-way ANOVA). **(e)** At 9 months, J20 mice showed memory deficits compared to the other three lines: WT, Casp2KO and J20/Casp2KO (7 male mice per group, * $p < 0.05$, two-way ANOVA). **(f)** Memory deficits persisted at 14 months of age (* $p < 0.05$, two-way ANOVA). **(g,h)** The four lines performed similarly in visible platform trials with regard to time to reach the platform **(g)** and speed **(h)**.

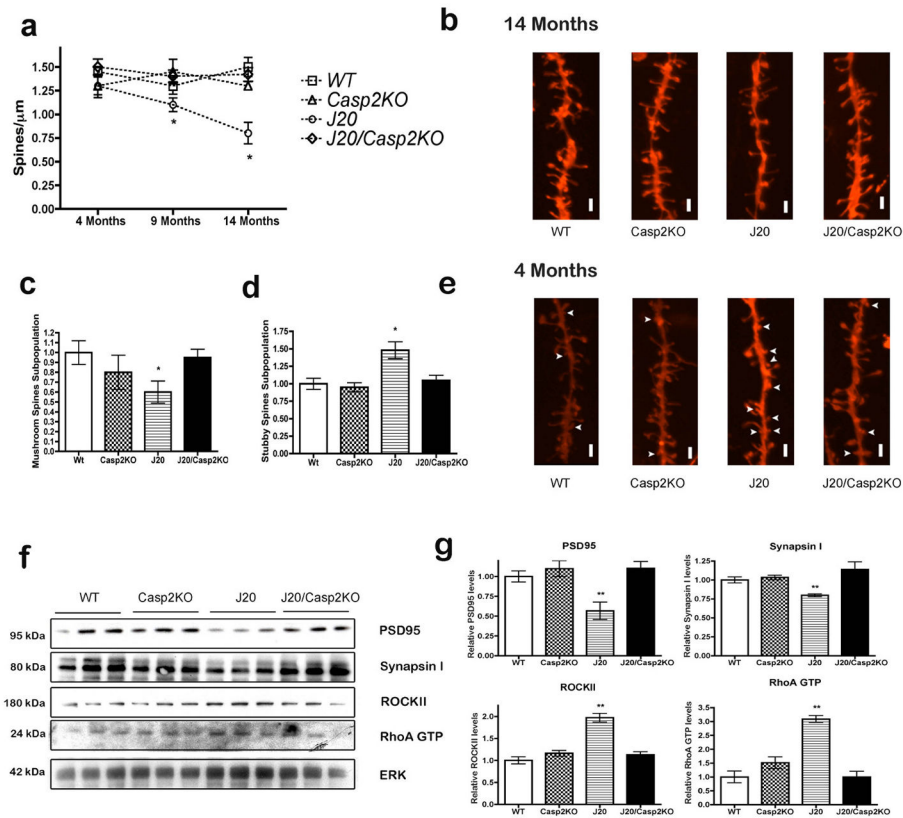


Figure 4. Dendritic spine loss in J20 mice is reversed in J20/Casp2KO animals

Mice from each line (WT, Casp2KO, J20 and J20/Casp2KO) were analyzed at 4, 9 and 14 months of age for spine changes. **(a)** J20 mice showed a significant decrease in spine density at 9 and 14 months of age compared to WT, Casp2KO and J20/Casp2KO mice. Data presented as the mean spine density \pm s.e.m. ($n=6$ mice, 50 dendrites per mouse; $*p<0.05$, two-way ANOVA) **(b)** Images of DiI-labeled dendrites and spine morphologies in hippocampal neurons from 14-month-old mice of each line. **(c)** J20 mice showed a significant decrease in mushroom spine subpopulation at 4 months of age, while J20/Casp2KO mice showed same levels as WT. Histogram showing the relative number of mushroom-type spines compared to WT mice. Data presented as the mean density \pm s.e.m. ($n=5$ mice, 50 dendrites per mouse, $*p<0.05$, two-way ANOVA). **(d)** J20 mice showed a significant increase in stubby spine subpopulation at 4 months of age, while J20/Casp2KO mice showed similar levels as WT. Histogram showing the relative density of stubby-type spines compared to WT mice. Data presented as the mean density \pm s.e.m. ($n=5$ mice, 50 dendrites per mouse, $*p<0.05$, two-way ANOVA). **(f)** Representative Western blots of hippocampal extracts from 14-month-old mice showing that alterations in synaptic and dendritic spine markers seen in J20 mice are absent in J20/Casp2KO mice ($n=10$ mice, $**p<0.01$, two-tailed Student's *t*-test). **(g)** Densitometric quantification of immunoblots in panel c. Levels of post- and pre-synaptic markers PSD95 and Synapsin-1 were reduced in J20 mice compared to WT and J20/Casp2KO mice ($**p<0.01$, two-tailed Student's *t*-test). Levels of ROCK-II and RhoA-GTP proteins were elevated in J20 mice compared to WT and

J20/Casp2KO mice (** $p < 0.01$, two-tailed Student's t -test). Histograms represent the densitometric mean \pm s.d. (n=10 mice).

Author Manuscript

Author Manuscript

Author Manuscript

Author Manuscript

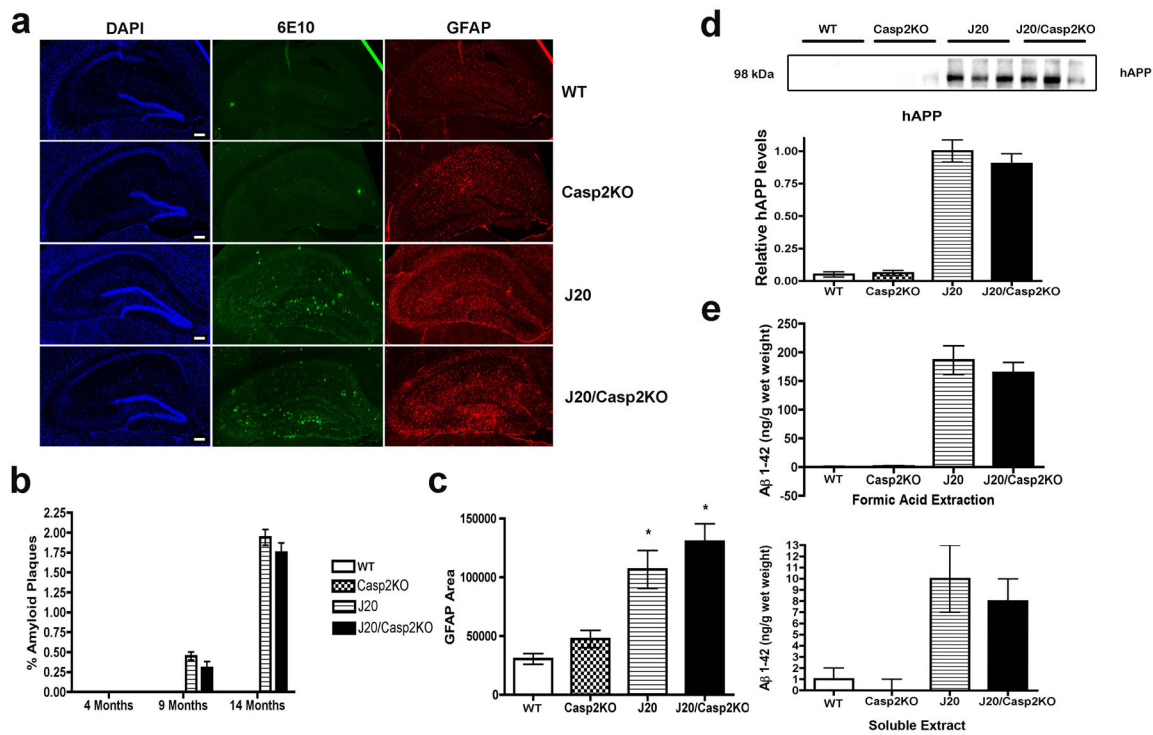


Figure 5. APP levels, amyloid plaque load and astrogliosis in J20 and J20/Casp2KO mice are similar

At least 6 mice from each genotype were used to study APP levels and amyloid load. **(a)** Representative images at 14 months of hippocampal slices stained with DAPI, Aβ (6E10) and GFAP antibodies. **(b)** Amyloid plaque load in each of the 4 lines was quantified at 4, 9 and 14 months of age using ImageJ. Data presented as the percentage relative to the total area of the hippocampal slice. **(c)** GFAP immunopositive areas were quantified using ImageJ. Both J20 and J20/Casp2KO had elevated levels compared to WT or Casp2KO mice. Data are presented as the mean ± s.d. (5 hippocampal slices per mouse were quantified, *p<0.05, one-way ANOVA). **(d)** Representative Western blot and densitometric analysis of protein extracts from mouse hippocampus showing similar levels of hAPP in both J20 and J20. Data presented as the mean ± s.d. **(e)** Hippocampal Aβ_{x-42} levels in both insoluble and soluble fractions were measured by ELISA. There were no significant differences between J20 and Casp2KO mice. Data presented as the mean ± s.d. (n=6 mice per line).

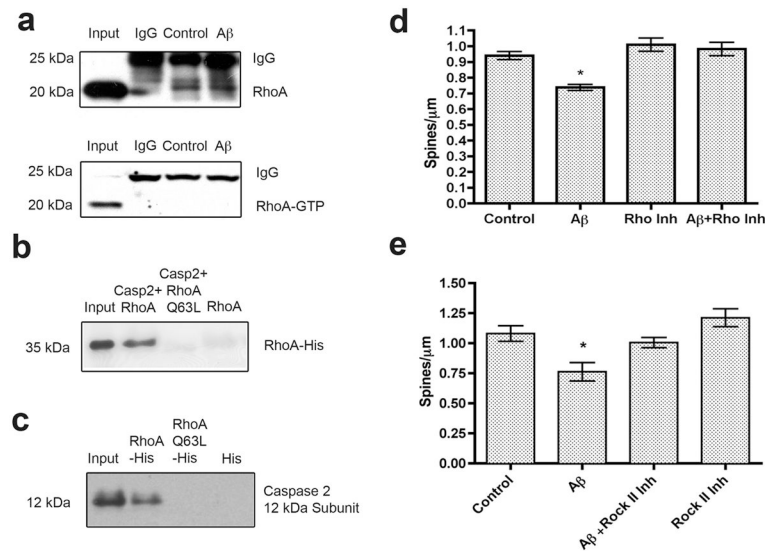


Figure 6. Inactive RhoA and caspase-2 form a complex

(a) Immunoprecipitation of caspase-2 in rat hippocampal neuron extracts with showing co-precipitation of RhoA but not RhoA-GTP in both Aβ-treated and control cells. (b) RhoA-His but not RhoA(Q63L)-His co-precipitated with recombinant caspase-2 using anti-caspase-2 antibody. (c) Co-precipitation of the caspase-2 12 kDa subunit with RhoA-His but not with constitutively active RhoA(Q63L)-His using Dy-nabead His-Tag beads. (d) Synaptosomes from rat hippocampus were pre-treated with bVAD-fmk prior to treatment with Aβ to trap active caspases. Treatment with either 300 nM or 1 μM Aβ led to activation of caspase-2. There was no caspase-2 activation in treated sonicated synaptosomes. (e) Inhibition of RhoA protects against Aβ-mediated spine loss. Rat hippocampal primary cultures were pretreated with 0.1 μg/ml of Rho inhibitor or with PBS for 15 minutes before treatment with 300 nM Aβ for 5h. Aβ treatment decreased spine number by 20% in cultures pretreated with PBS compared to control cultures while cultures pre-treated with the Rho inhibitor, C3 transferase, showed no spine loss compared to controls. Data presented as the mean ± s.e.m. (n=3 independent experiments, 150 dendrites per point, *p<0.05, one-way ANOVA). (f) ROCK-II inhibition protects against Aβ mediated spine loss. Rat hippocampal primary cultures were pretreated with 500 nM of ROCK-II inhibitor, Stemolecule or with PBS for 15 minutes before treatment with 300 nM Aβ for 24h. Aβ treatment decreased spine number by 40% in cells pretreated with PBS while cells pretreated with the ROCK-II inhibitor showed no loss compared with controls. Data presented as the mean ± s.e.m. (n=3 independent experiments, 50 dendrites per point, *p<0.05, one-way ANOVA).

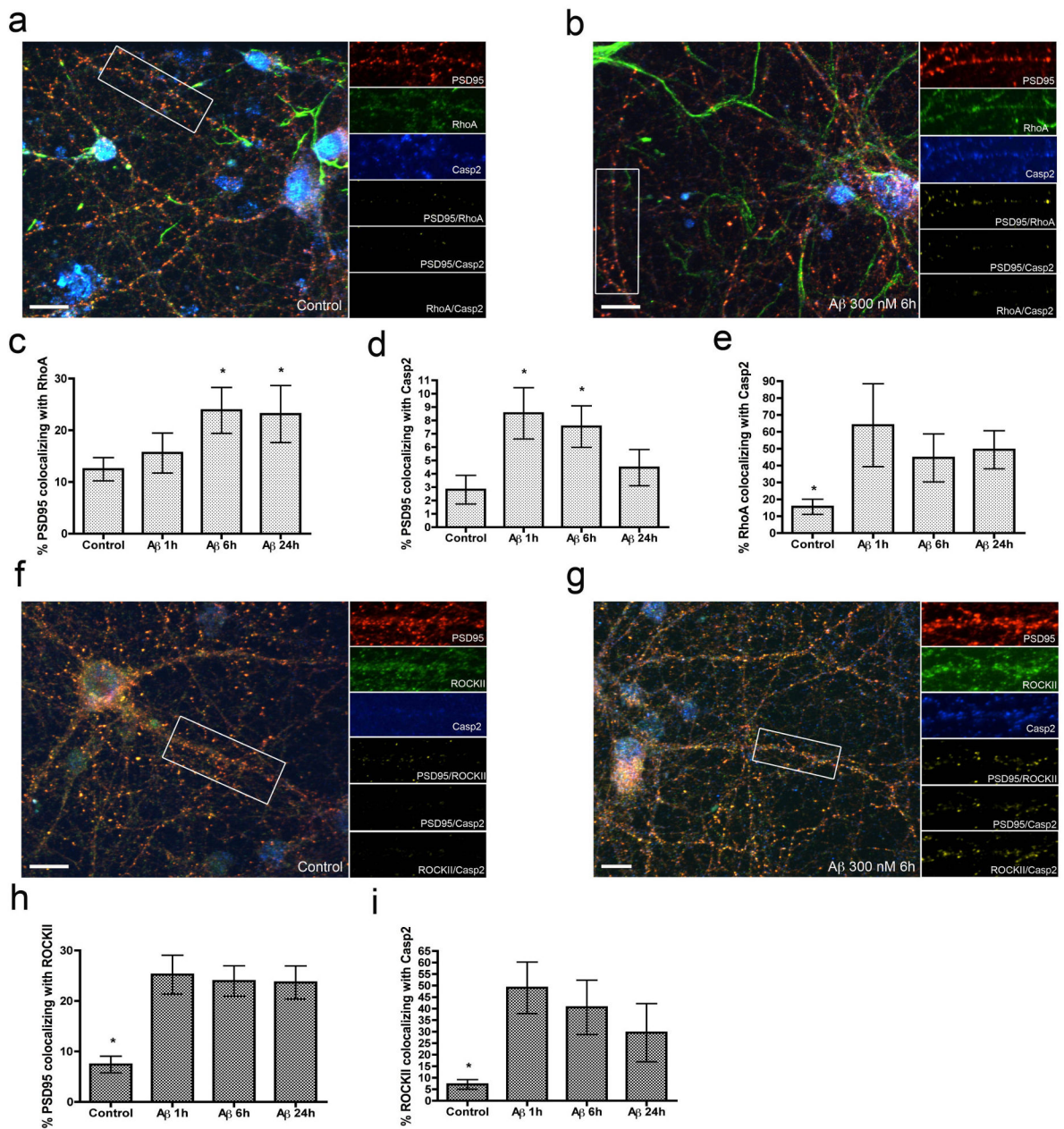


Figure 7. RhoA, ROCK-II and caspase-2 translocate to spines following A β treatment
(a) Representative confocal images of vehicle-treated cultures stained for PSD95 (Red), RhoA (green) and caspase-2 (blue). Higher magnification examination of a dendritic segment revealed that both RhoA and caspase-2 were present mainly in dendritic shafts. Colocalization of proteins is represented in yellow (analyzed with Velocity software; boxed areas showing enlarged den-dritic segments. Scale bar = 10 μ m). **(b)** Representative confocal images of culture hippocampal neurons treated for 6h with A β 300 nM and stained for PSD95 (Red), RhoA (green) and caspase-2 (blue). **(c)** Quantification of colocalization of RhoA with PSD95, represented as the percentage of PSD95 puncta colocalized with RhoA. Data presented as the mean \pm s.e.m. (n=3 independent experiments, *p<0.05, one-way

ANOVA). **(d)** Quantification of colocalization of caspase-2 with PSD95, represented as the percentage of the PSD95 puncta colocalized with RhoA. Data presented as the mean \pm s.e.m. (n=3 independent experiments, *p<0.05, one-way ANOVA). **(e)** Quantification of colocalization of caspase-2 with RhoA, represented as the percentage of the RhoA puncta colocalized with cas-pase-2. Data presented as the mean \pm s.e.m. (n=3 independent experiments, *p<0.05, one-way ANOVA). **(f)** Representative confocal image of an untreated hippocampal neuron stained for PSD95 (Red), ROCK-II (green) and caspase-2 (blue). Higher magnification of a dendritic segment revealed that both ROCK-II and caspase-2 were present mainly in dendritic shafts. Colocalization of proteins is represented in yellow (analyzed with Volocity software; boxed areas showing enlarged dendritic segments. Scale bar = 10 μ m). **(g)** Representative confocal image of a treated cultured hippocampal neuron (A β , 300 nM) stained for PSD95 (Red), ROCK-II (green) and caspase-2 (blue). **(h)** Quantification of colocalization of ROCK-II with PSD95, represented as the percentage of PSD95 puncta that colocalized with ROCK-II. Data presented as the mean \pm s.e.m. (n=3 independent experiments, *p<0.05, one-way ANOVA). **(i)** Quantification of colocalization of caspase-2 with ROCK-II, represented as the percentage of ROCK-II puncta colocalized with caspase-2. Data presented as the mean \pm s.e.m. (n=3 independent experiments, *p<0.05, one-way ANOVA).

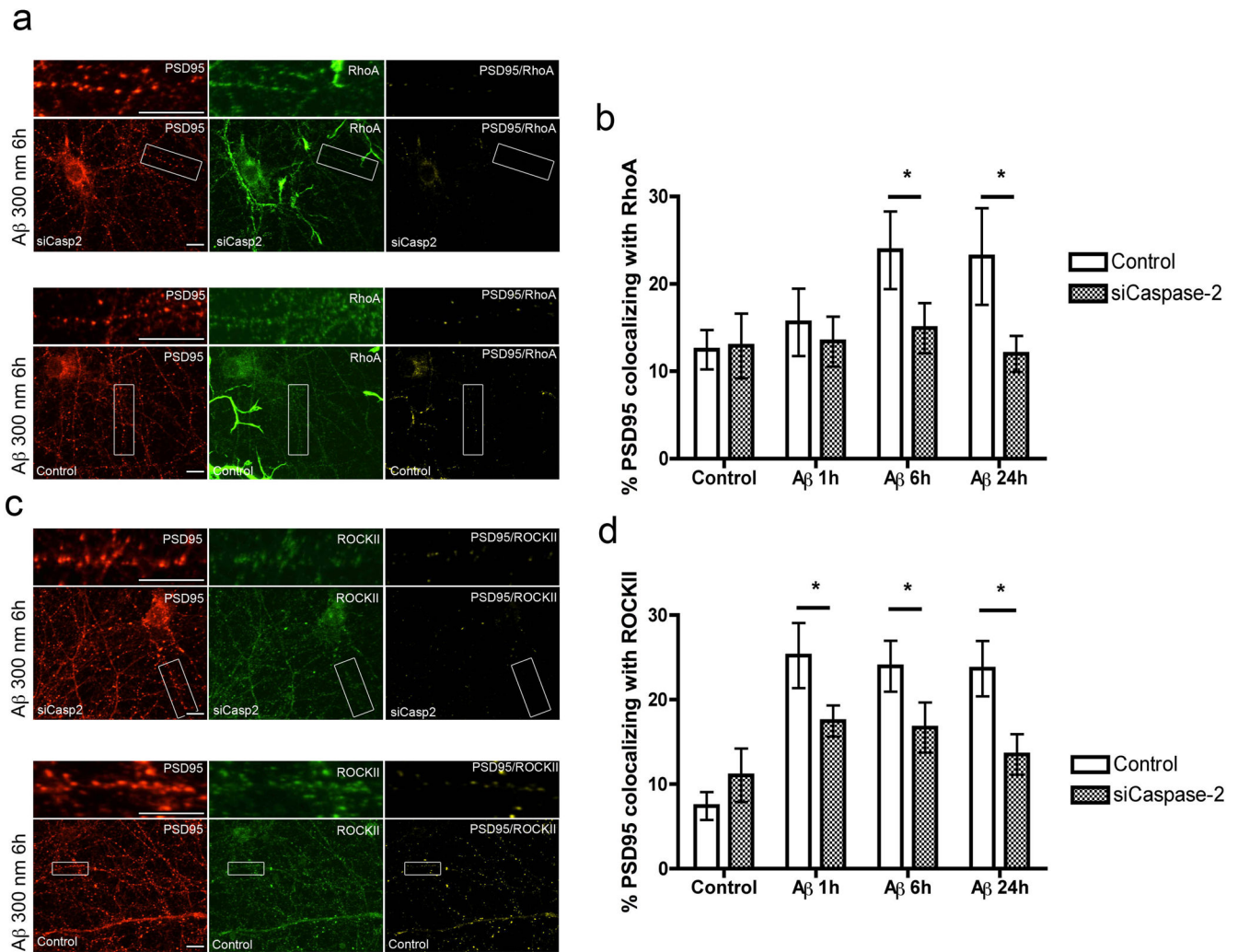


Figure 8. Aβ induced RhoA and ROCK-II translocation to dendritic spines is blocked by down-regulation of caspase-2

(a) Representative confocal images of hippocampal cultures stained for PSD95 (Red) and RhoA (green), pre-treated with siCasp2 or with vehicle (control) and treated for 6h with 300 nM Aβ. Colocalization of proteins is represented in yellow (analyzed with Volocity software; boxed areas showing enlarged dendritic segments. Scale bar = 10 μm). (b) Quantification of colocalization of RhoA with PSD95, represented as the percentage of PSD95 puncta colocalized with RhoA. Colocalization was measured prior to treatment with Aβ and at 1, 6 and 24h after treatment. Data presented as the mean ± s.e.m. (n=3 independent experiments, *p<0.05, one-way ANOVA). (c) Representative confocal image of a hippocampal neuron stained for PSD95 (Red) and ROCK-II (green) pretreated with siCasp2 or with vehicle and treated for 6h with 300 nM Aβ. Colocalization of proteins is represented in yellow (analyzed with Volocity software; boxed areas showing enlarged dendritic segments. Scale bar = 10 μm). (d) Quantification of colocalization of ROCK-II with PSD95, represented as the percentage of PSD95 puncta colocalized with ROCK-II. Colo-calization was measured prior to treatment with Aβ and at 1, 6 and 24h after treatment.

Data presented as the mean \pm s.e.m. (n=3 independent experiments, *p<0.05, one-way ANOVA).

Author Manuscript

Author Manuscript

Author Manuscript

Author Manuscript